JOURNAL OF VIROLOGY, Jan. 1991, p. 326–334
0022-538X/91/010326-09$02.00/0

Vol. 65, No. 1

Catalysis of Poliovirus VP0 Maturation Cleavage Is Not Mediated by Serine 10 of VP2

JAMES J. HARBER,[1]* JOHNATHAN BRADLEY,[1]† CARL W. ANDERSON,[2] AND ECKARD WIMMER[1]

Department of Microbiology, State University of New York at Stony Brook, Stony Brook, New York 11794,[1] and Department of Biology, Brookhaven National Laboratory, Upton, New York 11973[2]

Received 23 May 1990/Accepted 4 October 1990

The maturation of the poliovirus capsid occurs as the result of a single unexplained proteolytic event during which 58 to 59 copies of the 60 VP0 capsid protein precursors are cleaved. An autocatalytic mechanism for cleavage of VP0 to VP4 and VP2 was proposed by Arnold et al. (E. Arnold, M. Luo, G. Vriend, M. G. Rossman, A. C. Palmenberg, G. D. Parks, M. J. Nicklin, and E. Wimmer, Proc. Natl. Acad. Sci. USA 84:21–25, 1987) in which serine 10 of VP2 is activated by virion RNA to catalyze VP4-VP2 processing. The hypothesis rests on the observation that a hydrogen bond was observed between serine 10 of VP2 (S2010) and the carboxyl terminus of VP4 in three mature picornaviral atomic structures: rhinovirus 14, mengovirus, and poliovirus type 1 (Mahoney). We constructed mutant viruses with cysteine (S2010C) or alanine (S2010A) replacing serine 10 of VP2; these exhibited normal proteolytic processing of VP0. While our results do not exclude an autocatalytic mechanism for the maturation cleavage, they do eliminate the conserved S2010 residue as the catalytic amino acid.

The maturation cleavage of poliovirus occurs concomitantly with encapsidation of viral RNA by the capsid proteins VP3, VP1, and VP0, an *N*-myristoylated polypeptide with the structure Myr-NH-VP4-VP2-COOH (24). Infectious virions contain 60 copies each of VP3 and VP1, 58 to 59 copies of VP4 and VP2, and 1 to 2 copies of VP0. The candidate catalytic residue responsible for the cleavage of VP0 to VP4 and VP2 was assigned to serine residue 10 (S2010; amino acid numbering for each viral protein starts at 1001, 2001, 3001, and 4001 for VP1, VP2, VP3, and VP4, respectively) of the VP2 component of VP0 (2). Inspection of the three-dimensional structures of rhinovirus serotype 14 and mengovirus (picornavirus subgroups rhinovirus and cardiovirus, respectively), led Arnold et al. (2) to propose that S2010 mediated autocatalytic cleavage of VP0 via RNA-assisted catalysis. It was implied that the same mechanism applies to aphthovirus (foot-and-mouth disease virus) and to enterovirus (poliovirus). Arnold et al. (2) sought to build a unified hypothesis of VP0 cleavage on the basis of the correlation of an implied VP0 structural motif of four major picornaviral subgroups. The hypothesis was generated from atomic structures of mature viruses which had cleaved VP0 because molecular models of uncleaved VP0 were not available. The structural motif correlated in human rhinovirus 14 (22), poliovirus (10), and mengovirus (20) was a single hydrogen bond between S2010 of VP2 (serine 2011 of mengovirus) and the carboxyl-terminal residue of VP4 (N4069 of rhinovirus and poliovirus; A4070 of mengovirus). Recent refinements of rhinovirus structure (3) and mengovirus structure (15) still support the hypothesis of Arnold et al. (2). An arginine residue (R2012) of rhinovirus is also within hydrogen bonding distance of the carboxyl terminus of VP4 and is assigned the role of stabilizing the position of a nucleotide base which acts during catalysis (2). Interestingly, the R2012 side chain of poliovirus and mengovirus is in a distal configuration and not within hydrogen bonding distance in these cleaved structures. Although foot-and-mouth disease virus was included in the original hypothesis, it does not contain a homologous S2010 residue. The suggestion that foot-and-mouth disease virus serine 28 of VP2 might perform the same function (2) was not tenable since subsequently these residues were found to be more than 0.8 nm from the VP4 carboxyl terminus. The foot-and-mouth disease virus crystal structure therefore provides no evidence to support the hypothesis (1).

The picornavirus genome and the genome-length mRNA are translated to yield a single product, the polyprotein (13, 27). Capsid proteins are located in the amino-terminal section (designated P1; structurally, Myr-NH-VP4-VP2-VP3-VP1-COOH) of the polyprotein. In poliovirus, P1 is separated from the polyprotein during translation through a *cis* cleavage event catalyzed by 2A proteinase at its own amino terminus. After translation of the entire polyprotein reading frame, the proteinase 3CD is autocatalytically separated from the carboxyl end of the polyprotein. VP0, VP3, and VP1 are then released from P1 by 3CD proteinase-mediated cleavage (for review, see reference 9 and citations therein). VP0, VP3, and VP1 comprise 5S protomeric units which are capable of self associating to form 14S pentamers. Twelve pentameric units can self assemble to form 75S empty capsids or, in conjunction with plus-stranded poliovirus RNA linked to the peptide VPg, they can assemble to 150S virions (for a review, see reference 23). The coincident packaging of RNA and cleavage of VP0 has implicated the bases of polynucleotides in the cleavage mechanism. Self regulation of proteolytic processing remains an attractive mechanism for the maturation cleavage because, besides VP0, VP4, VP2, VP3, and VP1, no other protein has been found to exist in purified viral capsid preparations. The conservation of the VP4/VP2 proteolytic cleavage at a specific amino acid pair (in poliovirus, the asparagine-serine peptide bond [17]) implies a mechanism which is specific for a distinct peptide bond.

The mechanism for VP0 cleavage proposed by Arnold et al. (2) resembles that of the serine proteases. A nucleotide

* Corresponding author.
† Present address: Division of Biology, California Institute of Technology 216-76, Pasadena, CA 91125.

base of the encapsidated virion RNA takes the place of the histidine of the charge relay network. The conserved arginine (R2012) is assumed to have some role in the catalytic process by binding the phosphates of an RNA base, thus orienting it during the catalysis. In the first step of the proposed mechanism, a proton from the hydroxyl side chain of the catalytic serine is extracted by an amino group of the RNA base. This allows the serine alkoxide to nucleophilically attack the VP4-VP2 peptide bond. As in the case of the serine proteases, an oxyanion tetrahedral intermediate is formed. The tetrahedral intermediate is resolved by hydrolysis, and the carboxyl terminus of VP4 and the amino terminus of VP2 are released as the serine reextracts of proton from the RNA base. The reaction conclusion is analogous to the final step of the serine protease mechanism, where the charge relay network is reestablished as the serine reextracts a proton from the histidine residue of the catalytic triad.

The combination of nucleic acid and protein acting in concert during catalysis made the hypothesis by Arnold et al. (2) an attractive mechanism for the generation of mature picornaviral virions. In this report we have tested the hypothesis by constructing mutant viruses with a cysteine (S2010C) or an alanine (S2010A) in the place of S2010. While we recognize that the proposed catalytic serine is conserved evolutionarily among the known members of the rhinovirus, cardiovirus, and enterovirus genera, we find that eliminating the serine hydroxyl side chain (by replacement with a cysteine sulfhydryl or alanine methyl side chain) does not detrimentally affect VP0 cleavage or virus function to the degree expected.

MATERIALS AND METHODS

Mutagenesis of VP0. The construction of the poliovirus type 1 (Mahoney) [PV1(M)] cDNA subclone pBS+VP0 in the Bluescript M13 helper phage system (Stratagene, La Jolla, Calif.) has been described (14). pBS+VP0 spans the region of poliovirus nucleotide 70 in the 5′ untranslated region to nucleotide 1174 in VP2 and thus contains all 69 amino acids of the VP4 capsid protein and a 57-amino-acid segment of the 272-amino-acid VP2 capsid protein. pBS+VP0 yields packaged M13 single-stranded DNA that is of the same polarity as the virion plus-stranded (sense) RNA. Mutagenesis was accomplished by using mismatched (antisense) oligonucleotides (25) which changed the **AGC** (serine) codon at amino acid 10 of VP2 to a **TGC** cysteine (3′ CGCCCATA**A**C**G**CTATCTC 5′) and a **GCC** alanine (3′ CGCCCATA**C**G**G**CTATCTC 5′). By using the suggested nomenclature of Bernstein et al. (5), we have designated these mutations W1-1B-S2010C and W1-1B-S2010A. Uracil-substituted template for mismatch repair was prepared by using the method of Kunkel (16). Phosphorylation of oligonucleotides, primer extension with Klenow fragment, ligation, and transformation were accomplished by using the method of Zoller and Smith (29). The *Kpn*1-*Aat*II DNA fragment (nucleotides 70 to 1118) from mutated pBS+VP0 was cloned back into homologous sites in the full-length PV1(M) cDNA vector pT7XL which is derived from plasmid pT7 PV1-5 (28).

Isolation of mutant viruses and single-step growth curves. Full-length infectious RNAs of PV1(M) and the mutants were transcribed by T7 RNA polymerase from native PT7XL and PT7XL containing the alanine and cysteine mutations. The synthetic RNA was transfected onto HeLa cells by use of the DEAE-dextran method as described previously (28). After complete lysis of the transfected 100-mm HeLa cell monolayers (32 to 48 h), the virus was plaque purified three times. High-titer virus stocks were prepared from 1 liter of HeLa suspension cultures for subsequent use in experiments described below. Growth curves were determined by using the method described by Murray et al. (21).

Preparation and sequencing of viral RNA. Sixty-millimeter plates of HeLa R19 cell monolayers (4×10^6 cells) were infected with poliovirus in 200 μl of phosphate-buffered saline (PBS) at a multiplicity of infection of 25. The cells were gently rocked for 30 min, excess virus was removed, and 2 ml of DME plus 5% calf serum was added. The infected cells were incubated at 37°C with 5% CO_2. At 7.5 h postinfection, the monolayers were washed two times in cold PBS. A 400-μl volume of Nonidet P-40 lysis buffer (10 mM Tris [pH 7.5]–100 mM NaCl–1 mM EDTA–0.5% Nonidet P-40) was applied to the monolayer, and the cytoplasmic extract and nuclei were pipetted into a 1.5-ml microcentrifuge tube. The nuclei were pelleted at $1,000 \times g$ for 5 min in a microcentrifuge, and the supernatant was extracted with phenol-chloroform. The RNA was ethanol precipitated, dried, and suspended in 20 μl of water. A 2-μl volume was then analyzed on a gel by using a T7 transcript from the poliovirus cDNA clone as a marker. Typically, tRNA, 18S RNA, and 28S RNA bands were seen in lysate preparations in addition to the poliovirus RNA. A 5-μl volume of the preparation was used in RNA sequencing. An oligonucleotide, 50 bases downstream from the mutation with the sequence 3′ CCGCCGATTAAGTC 5′, was used as a primer for deoxynucleotide sequencing with avian myeloblastosis virus reverse transcriptase (Stratagene) by using the protocol of Kitamura et al. (13) and terminal transferase modifications (6).

Radiolabeling of poliovirus lysates and virions. PV1(M) and the cysteine and alanine mutant viruses were labeled as described by Lee et al. (19). The infected cells were harvested for lysate and virus preparations at 5 and 7 h postinfection, respectively. Lysate preparations were harvested by washing two times with PBS and then were treated with Nonidet P-40 lysis buffer for 5 min. Lysates were then spun in an Eppendorf centrifuge for 1 min at $12,000 \times g$. A 5-μl volume of the lysate was then trichloroacetic acid (TCA) precipitated and counted by scintillation. A sample of lysate corresponding to 10^5 cpm was used for analysis by sodium dodecyl sulfate-polyacrylamide gel electrophoresis (SDS-PAGE). The cells for viral particle analysis were washed with PBS at 7 h postinfection, scraped with a rubber policeman into 0.5 ml of reticulocyte standard buffer (RSB) plus Mg^{2+} (10 mM NaCl–10 mM Tris hydrochloride [pH 7.4]–1.5 mM $MgCl_2$), and lysed by three cycles of freezing and thawing. The cell lysate was spun at $3,000 \times g$ for 5 min to pellet membranes and nuclei. The supernatant was adjusted to 5 mM EDTA, 1% Sarkosyl, and 0.3 M NaCl and centrifuged through 5 ml of 30% sucrose at $100,000 \times g$ to pellet the virus (Beckman 50.2Ti rotor, 30,000 rpm, 3 h, 22°C). The sucrose was immediately decanted from the viral pellet, and the pellet was suspended in 100 μl of RSB plus Mg^{2+}. A 5-μl fraction was TCA precipitated, and samples containing 5×10^5 cpm were used for SDS-PAGE.

Separation of empty capsids and assembled virions. HeLa cell monolayers (100 mm) were labeled 3.5 h postinfection with 40 μCi of [^{35}S]methionine (ICN) per ml for 90 min as described previously (19). The cells were washed, and 750 μl of RSB plus Mg^{2+} containing 0.5% Nonidet P-40, 1 μM phenylmethylsulfonyl fluoride, and 30 U of RNasin

(Promega) was added. The cell lysate was spun at 3,000 × *g* for 5 min to pellet membranes and nuclei. A 700-μl volume of the cytoplasmic extract was loaded onto 15 to 30% sucrose gradients in RSB plus Mg^{2+}. The three samples were centrifuged at 28,000 rpm for 3 h in an SW41 rotor and pumped into equivalent fractions. TCA-precipitable materials contained in the fractions were determined by applying a 5-μl sample on a Whatman GF/C glass fiber 2.4-cm filter. The filters were subsequently immersed in 1 liter of ice-cold 10% TCA, agitated for 15 min, washed two times in 1 liter of 70% ethanol for 5 min, dried under a heat lamp, and counted by scintillation (25). Equal volumes of each fraction were run on SDS-polyacrylamide gels to determine the ratio of empty capsids to mature virions and assay the extent to which virion proteins were separated from empty capsids.

Amino-terminal sequencing of VP2 proteins. HeLa cell monolayers (100 mm) were infected as above except that, at 3 h postinfection, the wild-type virus was labeled with 250 μCi of [^{3}H]serine (New England Nuclear Corp., Boston, Mass.) in 2 ml of minimal essential medium, the cysteine mutant was labeled with 250 μCi of [^{35}S]cysteine (ICN) in 2 ml of minimal essential medium lacking cysteine, and the alanine mutant was labeled with 250 μCi of [^{3}H]alanine (New England Nuclear) in 2 ml of minimal essential medium. All media formulations contained 5 μg of dactinomycin per ml. The viruses were separated from empty capsid components and pentameric units in 15 to 30% gradients as described above. The viral peaks were pooled, the sucrose concentration was diluted to 5% with RSB plus Mg^{2+}, and the sample was spun at 30,000 rpm in a Beckman 50.2Ti rotor for 3 h to pellet the virus. The supernatant was decanted, and the virus pellet was dried under vacuum. The virus was subsequently suspended and boiled for 5 min in Laemmli loading buffer (17). Assembled viral proteins VP1, VP2, VP3, and VP4 from [^{3}H]serine, [^{35}S]cysteine, and [^{3}H]alanine samples were separated on 45-cm-long SDS-polyacrylamide gels, and the VP2 band was rehydrated in the sample chamber of an electroelution device (ISCO, Lincoln, Neb.). The chamber buffer was 50 mM NH_4HCO_3–0.02% SDS, and the sample cup buffer was 10 mM NH_4HCO_3–0.02% SDS. The electroelution was performed at 3 W constant power for 4 h. Radioactive VP2 samples were applied to the spinning cup of a Beckman 890M protein sequencer directly in the electroelution buffer as described previously (17, 26). A 50-μg amount of unlabeled apomyoglobin was loaded in the spinning cup with each sample to serve as an internal sequencer performance standard. Each Edman cycle residue was dissolved in 300 μl of 50% methanol; 150 μl was mixed with 3 ml of Aquasol II (New England Nuclear), and the radioactivity was determined in a scintillation counter. A portion of the remainder was analyzed by reverse-phase high-pressure liquid chromatography to verify the phenylthiohydantoin-amino acid released from apomyoglobin.

Computer methodology. Coordinates for the viruses described were obtained from the Brookhaven Protein Databank (Upton, N.Y.), with the exception of those for poliovirus which were obtained from J. Hogle. The protein data bank access numbers for rhinovirus and mengovirus were 4RHV and 1MEV, respectively. Displays were generated on a Silicon Graphics IRIS personal workstation (Mountain View, Calif.) running the program INSIGHT (BIOSYM Technologies, Inc., San Diego, Calif.) and on an Evans and Sutherland PS390 (Salt Lake City, Utah) running FRODO version 6.6 (obtained from Rice University, Houston, Tex.) which was originally authored by T. A. Jones (11).

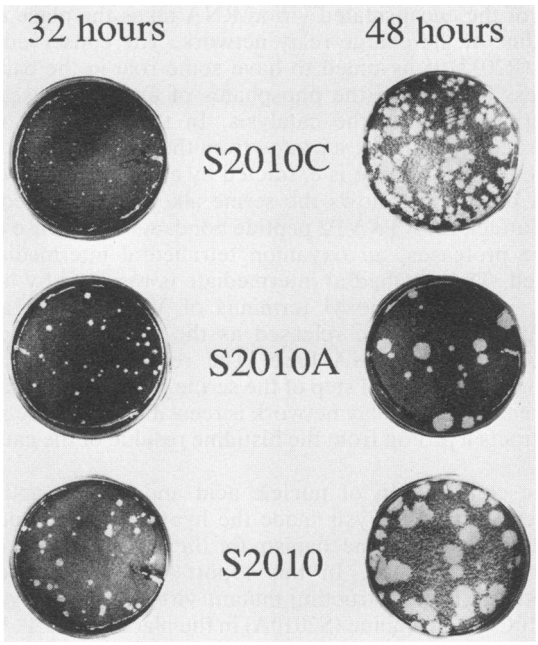

FIG. 1. Plaque phenotypes of S2010C, S2010A, and S2010 at 32 and 48 h. The cysteine mutant always exhibited a small-plaque phenotype. The alanine mutant plaque size is slightly smaller than that of the wild type, and an abundance of small plaques is present.

RESULTS

Isolation of mutant viruses. Site-directed mutagenesis of the serine residue 10 of VP2 (S2010) by using a subclone of the cDNA of PV1(M) produced S2010C and S2010A variant cDNAs as described in Materials and Methods. We verified the nucleotide changes by DNA sequencing prior to the construction of full-length cDNA clones and transcription with T7 polymerase in vitro. Upon transfection of HeLa cell monolayers with the full-length viral transcripts, cytopathic effect developed within 32 h for wild-type pT7XL whereas the S2010C and S2010A mutants required longer incubations (48 to 72 h) for complete cytopathic effect. We expected these differences because of our experience with other capsid mutant viruses (21). RNA prepared from HeLa R19 cells infected with 3× plaque-purified mutant viruses (S2010C and S2010A) and wild type (S2010) was sequenced to confirm that the cysteine, alanine, and serine codons were maintained in the appropriate viruses (S2010C, S2010A, and S2010, respectively) during virus propagation (data not shown).

Growth characteristics of mutants S2010C and S2010A. Plaque morphology of S2010A and S2010 (wild-type) viruses were found to be nearly indisinguishable at 32 h, whereas the S2010C virus displayed a characteristic small-plaque morphology (Fig. 1). At 48 h, S2010C small plaques were easily identified when compared with S2010 and S2010A large plaques. Wild-type PV1(M) plaques were characteristically both large and small at 48 h. The S2010A mutant displayed large plaques of a slightly smaller diameter than S2010 at 48 h, and there was an increased occurrence of small plaques. The growth kinetics of mutant viruses were assayed in 10-h growth curves (Fig. 2). S2010A and S2010C appeared to slightly delay viral eclipse as illustrated by their higher titers at time 0 to 2 h. We suspect that this delay is indicative of a defect in uncoating which is correlated with slow VP0

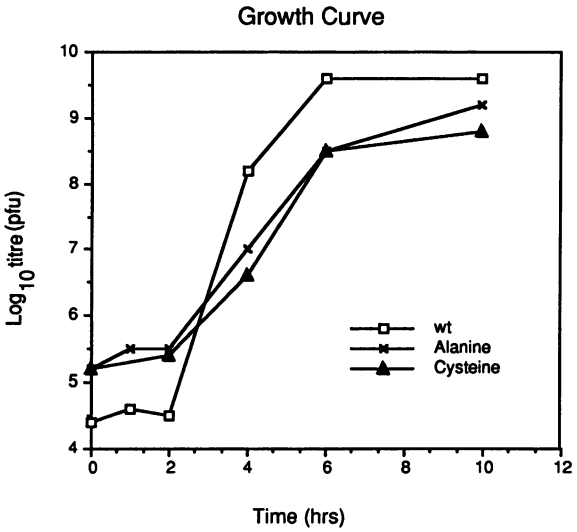

FIG. 2. Growth curve of wild-type (S2010), alanine (S2010A), and cysteine (S2010C) polioviruses. PFU are plotted as a function of time (hours). A multiplicity of infection of 25 PFU per cell was applied to 10^6 cells in 60-mm dishes and harvested at the time points (in hours) indicated by the symbols.

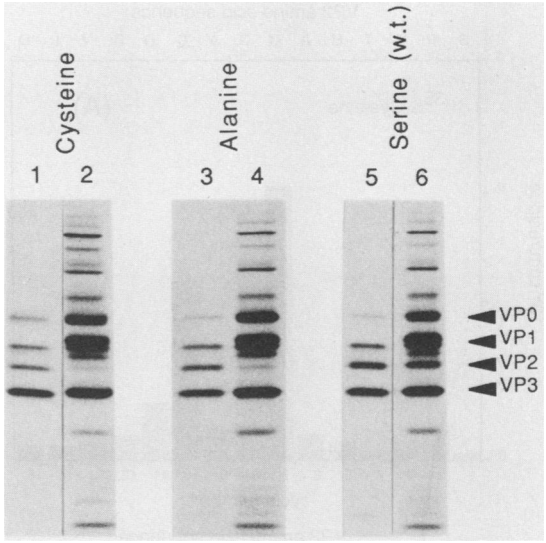

FIG. 3. Autoradiogram of SDS-PAGE of proteins labeled with [^{35}S]methionine after infection of HeLa R19 cells with wild-type and mutant viruses. Cysteine, alanine, and serine refer to the S2010C mutant, the S2010A mutant, and PV1(M), respectively. Lanes 1, 3, and 5 show capsid polypeptides of purified virions; lanes 2, 4, and 6 illustrate poliovirus-specific polypeptides seen in lysates of infected cells at 5 h. Shown are the 5×10^5 cpm of [^{35}S]methionine-labeled sample applied to each lane.

cleavage. Both mutants replicated to titers that were lower than that of wild-type virus at 37°C, while the yield of the S2010C mutant was reduced by a factor as high as 10 (Fig. 2). The mutant viruses were checked for temperature sensitivity at 32 and 39°C by using the attenuated Sabin virus and wild-type PV1(M) as controls. No dramatic difference in the titer of mutants S2010A and S2010C was observed at either temperature (data not shown). In addition, we found no variation in particle-to-PFU ratios for the mutant viruses S2010A and S2010C compared with wild-type poliovirus (data not shown).

Capsid polypeptides of the mutant viruses. When examined by SDS-PAGE, both mutant viruses showed patterns of capsid polypeptides similar to PV1(M) (Fig. 3, lanes 1, 3, and 5), an observation indicating that processing of the capsid precursors P1 to VP1, VP2, VP3, VP4, and VP0 had occurred regardless of the cysteine or alanine residues in position 10 of VP2. The S2010C virions reproducibly had more uncleaved VP0 relative to the other capsid proteins than wild-type or S2010A virions (Fig. 3, lanes 1 and 2). Lysates of infected cells analyzed at 5 h postinfection showed detectable differences in VP0 processing to VP2 (VP4 is not visible in Fig. 3). While levels of other capsid-specific polypeptides were comparable at this stage of infection, VP2 of S2010A and S2010C (Fig. 3, lanes 2 and 4) had not accumulated to the same extent as wild-type VP2 (Fig. 3, lane 6).

Sequence analysis of VP2. Although RNA sequencing verified the genetic changes in S2010C and S2010A (data not shown), we also confirmed the changed amino acid in position 10 of VP2 by direct sequence analysis. For this purpose, infections were carried out in the presence of one of three labeled amino acids, [^{3}H]serine (wild type), [^{35}S]cysteine, and [^{35}H]alanine. First, the N-terminal amino acid sequence of VP2 was analyzed with protein isolated from infected lysates. The profiles of radioactive amino acids released during Edman degradation are shown in Fig. 4. Capsid protein VP2 displayed the expected radioactive peaks at each sequence cycle (where the labeled amino acids in positions other than position 10 served as convenient controls for the labeling). Similar sequence data were obtained with VP2 isolated from sucrose gradient-purified virions (data not shown). These results confirmed that the amino acids at position 2010 of VP2 of the S2010C and S2010A viruses were in fact those that were introduced by genetic engineering.

Sedimentation of empty capsids and virions. Figure 5 illustrates SDS-PAGE analysis of individual fractions of 15 to 30% sucrose gradients for the cysteine and alanine mutants as compared with PV1(M). As can be seen, both mutant viruses display a pattern of mature virus (Fig. 5A and C, fractions 3 to 7; Fig. 5B, fractions to 5 to 9) and empty capsids (Fig. 5A and C, fractions 11 to 13; Fig. 5B, fractions 14 and 15) similar to that of PV1(M). Thus, processing of VP0 to VP4 and VP2 had occurred in the mature virion regardless of the presence of a cysteine or alanine in position 10 of VP2. However, it appeared that both mutant virions contained slightly more uncleaved VP0, an observation already made on inspection of Fig. 3. Moreover, the ratio of empty capsids to virions remained constant as measured by TCA-precipitated radioactivity found in the 160S and 75S peaks of the sucrose gradients (data not shown).

DISCUSSION

The experiments described above were designed to test a hypothesis by Arnold et al. (2) which predicted the involvement of amino acid S2010 in the maturation cleavage of poliovirus and other picornaviruses. Initially, we changed S2010 to cysteine (mutant S2010C), an amino acid whose side chain is larger than that of serine but whose sulfhydryl group could conceivably participate in the hydrolysis of the N-S pair between VP4 and VP2. Indeed, the viability of the S2010C mutant left open the possibility that a cysteine proteaselike mechanism could function in VP0 cleavage

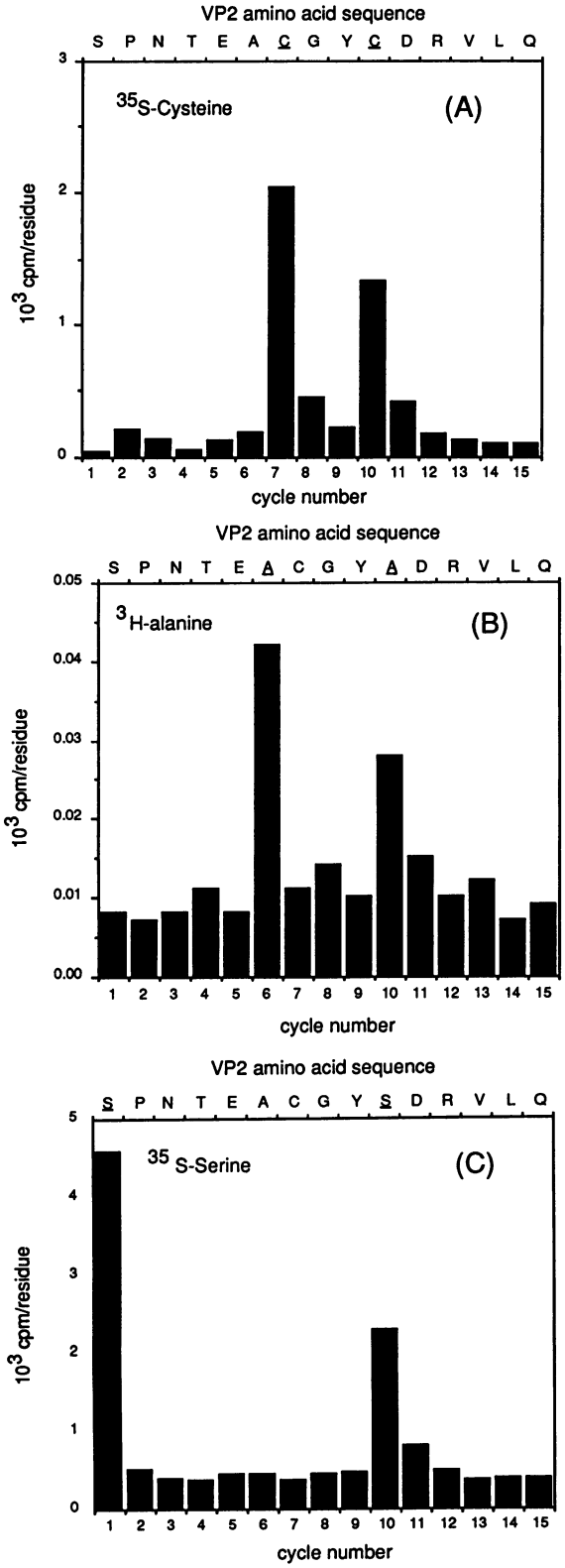

FIG. 4. Amino-terminal analysis of VP2 from wild-type and mutant viruses. The radioactivity released during the stepwise degradation of VP2, purified from infected cell extracts, is graphed. (A) [^{35}S]cysteine-labeled VP2 from mutant S2010C-infected cells (55,000 cpm applied); (B) [^{3}H]alanine-labeled VP2 from mutant S2010A-infected cells (9,100 cpm applied); (C) [^{3}H]serine-labeled VP2 from wild-type-infected cells (104,000 cpm applied). The expected N-terminal sequence is given at the top of each panel (13, 17); radiochemically detected residues are underlined. Similar results were obtained for VP2 isolated from purified virions (data not shown).

since viable virus was recovered. Catalytic activity of an alanine residue in position 10 of VP2 cannot be envisioned. We subsequently found viable S2010A mutants that did not display any grossly aberrant phenotype (for example, a virus that did not cleave VP0).

By showing that VP0 cleavage is allowed by the S2010C and S2010A mutants, we have ruled out the S2010 residue as an essential catalytic active-site amino acid. Indeed, we also rule out the involvement of this residue as a primary determinant of the cleavage site and thus of the cleavage specificity. Amino-terminal analysis of VP2 again confirmed serine as the first (2001) and tenth (2010) residues (17). A variety of cleavage products are not observed during amino-terminal analysis of VP0 mutants S2010C and S2010A because the release of radioactivity is confined to single cycles which correlate exactly with the protein sequence. Specificity of VP0 cleavage at the asparagine-serine peptide bond is maintained in the S2010A and S2010C mutants. All of this evidence eliminates the S2010 hypothesis in maturation cleavage.

If the serine in position 10 of VP2 is not involved catalytically in the maturation cleavage of poliovirus, are there other candidate amino acids nearby that could function in this process? A planar representation of VP4 carboxyl-terminal residues 4053 to 4069 and VP2 amino-terminal residues 2005 to 2016 from the poliovirus virion crystal structure (10) is illustrated in Fig. 6. The residues illustrated are located roughly near the threefold axis (at the intersection of three pentameric units of the virion). The amino terminus of VP2 is disordered in the crystal structure as is evidenced by the lack of correct peptide bonds for residues 2005 and 2006 and the absence of residues 2001 to 2004 (10). VPg-linked virion RNA is packed inside the capsid but is not represented in picornaviral crystal structures because its conformation is randomized among the many virions of the crystal (this problem occurs with all picornaviral structures analyzed to date).

The region depicted in Fig. 6 illustrates the residues principally cited in the hypothesis of Arnold et al. (2). These amino acids were analyzed by using the "hbond" command of the INSIGHT program. This command predicts hydrogen bonds when the distance between the proton on the donor atom and the heavy atom acceptor is less than a critical distance (0.24 nm); between donor and acceptor atoms 0.31 nm is the distance criteria. Angular criteria also define hydrogen bonding. The C=O carbonyl is approximately colinear with the hydrogen bond whereas the O—H bond makes an angle of about 120° with the C—O acceptor atom. The only two hydrogen bonds predicted by the program INSIGHT to exist in this region are shown in Fig. 6. As expected, a 0.289-nm bond exists between N4069 and S2010 (2, 22). However, a second hydrogen bond of 0.284 nm is predicted between the aspartic acids in position 11 of VP2 and aspartic acid 59 of VP4. This hydrogen bond is not predicted in rhinovirus 14, although by hypothetical rotation of the carbon alpha-carbon beta bond (X1) of D4059, the two aspartates can be brought into hydrogen bonding proximity. Thus the structure of VP2 and VP4 is conserved three

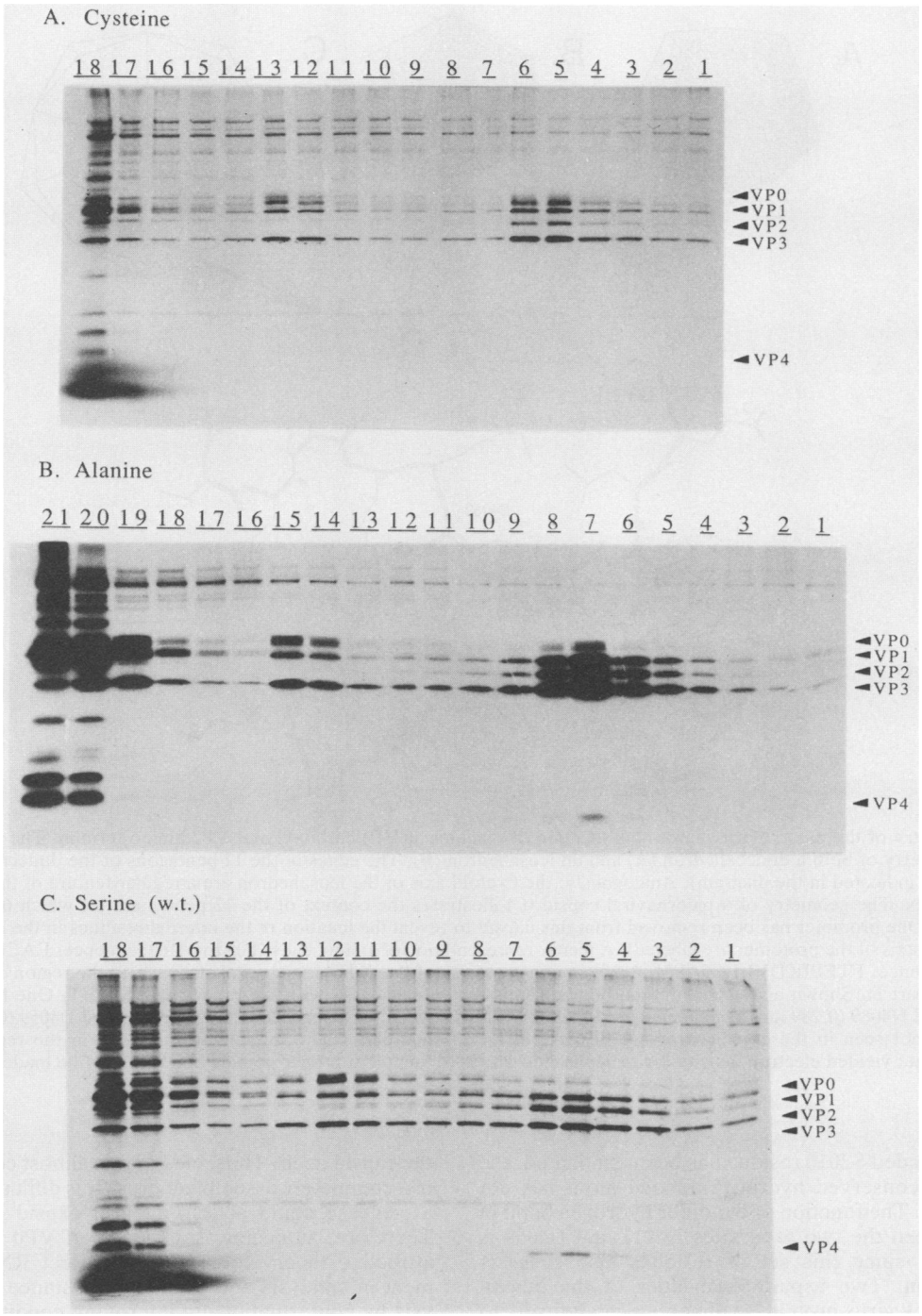

FIG. 5. Autoradiogram of SDS-PAGE of proteins from consecutive fractions containing [^{35}S]methionine-labeled cell extracts of virus-infected cells after zonal sedimentation on 15 to 30% sucrose gradients. Sedimentation is shown from left to right. The 150S virion peaks are concentrated in lanes 4 to 7 (cysteine mutant), lanes 5 to 9 (alanine mutant), and lanes 3 to 7 (wild-type virus). Empty capsids (75S) are concentrated in lanes 11 to 14 (cysteine), 13 to 16 (alanine), and 10 to 13 (wild type). The 5S pentamers sediment just below the top of the gradient (for example, see lane 19 of the alanine mutant). These gradients were made without detergent (to avoid degradation of labile particles), and consequently a large amount of nonstructural proteins is seen in the fractions.

dimensionally to some extent in this region. After VP0 cleavage, rhinovirus 14 has a hydrogen bond from residue R2012 to the carboxyl-terminal residue N4059. While the cleaved conformation of VP4 varies between families of viruses, in every case examined so far the carboxyl terminus of VP4 is close to the amino terminus of VP2 in the mature virus crystal structure.

What is the significance of the hydrogen bonding of poliovirus residues S2010 and D2011 (and R2012 in rhinovirus) to VP4 after cleavage? While catalytic involvement of

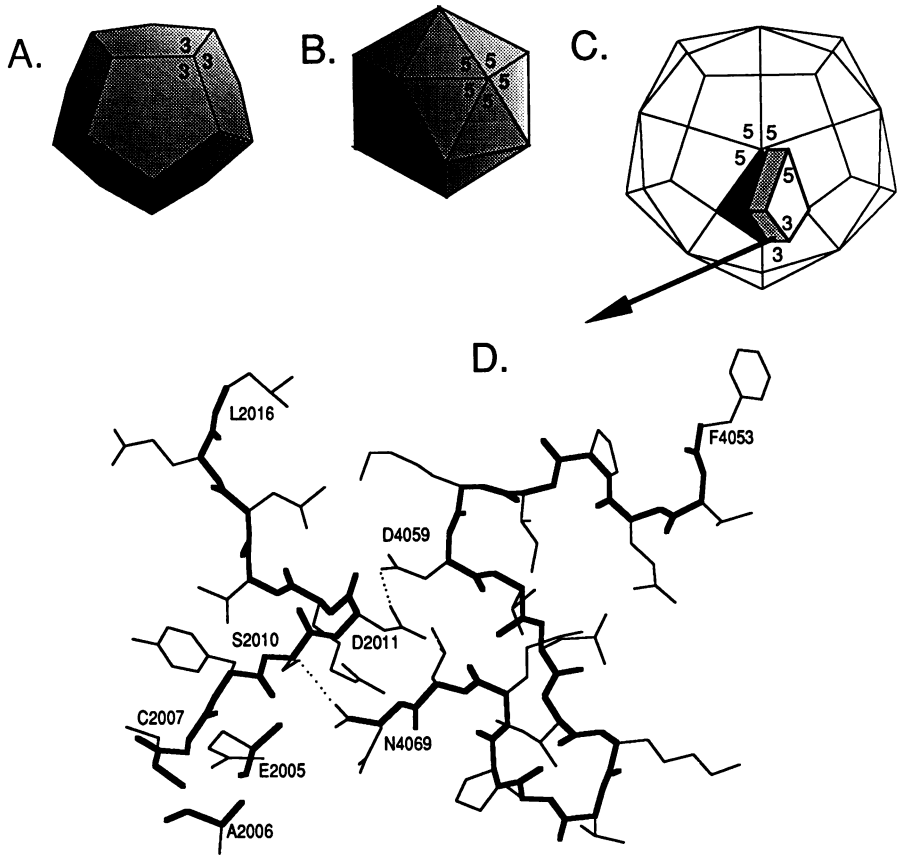

FIG. 6. Geometry of the picornavirus virion and location of residues at VP4 carboxyl and VP2 amino termini. The picornavirus capsid exhibits the symmetry of both a dodecahedron (A) and an icosahedron (B). The edges of the 12 pentagons of the dodecahedron (A) meet at the threefold axis (indicated in the diagram). Analogously, the fivefold axis of the icosahedron are a regular feature of the intersection of its 10 triangular planes. The geometry of a picornaviral capsid (C) illustrates the context of the 12 pentamers (of which 6 are visible) and 60 protomeric units. One promoter has been removed from this capsid to reveal the location of the internal residues in the region of S2010 (the five- and threefold axis of the protomer are labeled). A planar representation of amino acids 2005 to 2016 (sequence: EACGYSDRVLQL) and 4053 to 4069 (sequence: FTEPIKDVLIKTAPMLN) from one protomer of the poliovirus crystal structure in the region of the threefold axis are illustrated in part D. Shown also are hydrogen bonds in this region calculated with the program INSIGHT. One hydrogen bond falls between S2010 and N4069 (0.289 nm) as expected, and the other falls between two aspartate residues D2011 and D4059 (0.284 nm). Residues 2001 to 2004 are not seen in the crystal structure because of an absence of recognizable electron density in the region. Note that the crystallographic data yielded electron density for residues 2005 and 2006 such that proper peptide bonds cannot be made with the rest of the VP2 protein.

the hydrogen-bonded S2010 residue has been eliminated, the meaning of the conserved hydrogen-bonded motif has not been deciphered. The function of the other hydrogen bond in poliovirus between the two aspartates D2011 and D4059 is also a mystery, since this set of residues also suggests catalytic function. Two aspartate residues of the human immunodeficiency virus proteinase dimer act catalytically to cleave its substrate polyprotein into constituent functional subunits (an arginine also functions in the region of cleavage in the human immunodeficiency virus example although a mechanistic model for aspartyl proteinase action has not been formulated). Neither amino acid chain of poliovirus near D2011 nor that near D4059 contains the consensus amino acid sequence DTG (conserved among aspartyl proteases). Nevertheless, mutagenesis of D2011, D4059, and R2012 is in progress to investigate the role these residues have in virion morphogenesis. The proximity of amino-terminal VP2 and carboxyl-terminal VP4 residues and the hydrogen bonding in this region must reflect the fact that extensive migration of the cleaved residues is constrained by the capsid itself. Thus, cleavage is almost certainly occurring in a completely assembled virus. It is difficult to imagine how a protease could access internal capsid residues of VP0. Therefore, autocatalytic cleavage of VP0 remains the most attractive theory for cleavage. Direct RNA base involvement in catalysis and chemical assistance of RNA in catalysis by conformationally improving conditions for cleavage remain alternative mechanisms of RNA function during VP0 cleavage.

Hydrogen bonding in the VP4-VP2 region after cleavage must then serve some other function. This cleavage paradigm is consistent with the interpretation that the VP0 cleavage stabilizes the poliovirus capsid by modulating the formation of a seven-stranded β-sheet composed of components of adjacent pentamers as suggested by Filman et al. (8). Limited migration of the carboxyl terminus of VP4 and the amino terminus of VP2 from the active site after VP0 cleavage, with the function of stabilizing the threefold axis of pentamers surrounding encapsidated RNA, is an attractive theory for VP0 cleavage.

Compton et al. have demonstrated that a poliovirus containing a single point mutation coding for an amino acid change in VP2 fails to cleave VP0 and accumulates provirions (4). The mutant, designated VP2-103, contains a glutamine instead of arginine at position 76. The results suggest that VP0 packaging can be uncoupled from VP0 cleavage. The mutant codes for an amino acid change whose location is distal to the actual site of the cleaved VP0 residues. Consequently, the chemical influence of this change on cleavage awaits further investigation. A provirionlike virus is an ideal subject for crystallographic analysis of the uncleaved bond, since conformational rearrangements of the virus structural proteins accompanying RNA packaging could be elucidated.

The influence of amino-terminal VP1 residues adjacent to VP4 have recently been shown to be important for encapsidation and release of viral RNA (12). While the VP1 mutations (termed VP1-101 and VP1-102) are expected to be involved in virion morphogenesis, a mechanism has not been proposed for their involvement although the externalization of amino-terminal VP1 residues mediates the binding of poliovirus to liposomes (7). The viral eclipse and uncoating, which is accompanied by the loss of VP4, is then intimately tied to the fate of the amino terminus of VP1. These data collectively suggest that not only uncoating but also packaging of RNA may be a membrane-associated event.

Through site-directed mutagenesis, we expect to find a region of the poliovirus capsid which contains active-site amino acids specialized to maintain precise cleavage at the asparagine-serine peptide bond. The requirements for cleavage must include not only capsid amino acids (and possibly RNA nucleotide bases) which act catalytically but also a three-dimensional context for specificity of cleavage. At the present time, we are limited to viral structures in which VP0 is already cleaved. While our investigation of the residues which are in proximity to the cleaved VP4-VP2 bond continues, molecular modeling of a possible translocation of the VP2 amino terminus and VP4 carboxyl terminus towards a site of the interior of the capsid is being explored to identify other residues which may serve a catalytic role and would allow proteolytic specificity and timing of VP0 cleavage to RNA encapsidation.

ACKNOWLEDGMENTS

We are grateful to M. Rossmann for numerous discussions and assistance with programs and techniques for the display of icosahedral viruses. We thank J. Hogle for access to the coordinates for poliovirus prior to submission to the Brookhaven Data Bank, R. Butz for μVax, Unix, and PS390 system management, M. de Crombrugghe for development and instruction in programming resources, and J. Pflugrath for PS390 programming of symmetry operations particular to icosahedral viruses. N. Alonzo assisted with protein sequencing, A. Kameda assisted with tissue culture, P. Kissel helped with oligonucleotides, and C. Helmke helped with photography. We are grateful to C. K. Lee, J. Romero, H.-G. Kräusslich, and M. Nicklin for suggestions, clones, and cultures necessary to begin this work.

This work was supported in part by U.S. Public Health Service grants AI-15122 and CA-28146 to E. Wimmer and UO1 AI26049 to C. W. Anderson. C. W. Anderson was also supported by the Office of Health and Environmental Research of the U.S. Department of Energy. J. J. Harber was supported by Public Health Service training grant 5T32GM07964-07 from the National Institutes of Health and is a member of the Genetics Program of the State University of New York at Stony Brook in conjunction with the Cold Spring Harbor Laboratory and the Brookhaven National Laboratory.

REFERENCES

1. **Acharya, R., E. Fry, E. Stuart, G. Fox, D. Rowlands, and F. Brown.** 1989. The three-dimensional structure of foot-and-mouth disease virus at 2.9 Å resolution. Nature (London) **327**:709–716.
2. **Arnold, E., M. Luo, G. Vriend, M. G. Rossmann, A. C. Palmenberg, G. D. Parks, M. J. Nicklin, and E. Wimmer.** 1987. Implications of the picornavirus capsid structure for polyprotein processing. Proc. Natl. Acad. Sci. USA **84**:21–25.
3. **Arnold, E., and M. G. Rossmann.** 1990. Analysis of the structure of a common cold virus, human rhinovirus 14, refined at a resolution of 3.0 Å. J. Mol. Biol. **211**:763–801.
4. **Compton, S. R., B. Nelson, and K. Kirkegaard.** 1990. Temperature-sensitive poliovirus mutant fails to cleave VP0 and accumulates provirions. J. Virol. **64**:4067–4075.
5. **Bernstein, H. D., P. Sarnow, and D. Baltimore.** 1986. Genetic complementation among poliovirus mutants derived from an infectious cDNA clone. J. Virol. **60**:1040–1049.
6. **Deborde, D. C., C. W. Naeve, M. L. Herlocher, and H. F. Maassab.** 1986. Resolution of a common RNA sequencing ambiguity by terminal deoxynucleotidyl transferase. Anal. Biochem. **157**:275–282.
7. **Fricks, C. E., and J. M. Hogle.** 1990. Cell-induced conformational change in poliovirus: externalization of the amino terminus of VP1 is responsible for liposome binding. J. Virol. **64**:1934–1945.
8. **Filman, D. J., R. Syed, M. Chow, A. J. Macadam, P. D. Minor, and J. Hogle.** 1989. Structural factors that control conformational transitions and serotype specificity in type 3 poliovirus. EMBO J. **8**:1567–1579.
9. **Hellen, C. U., H. G. Kräusslich, and E. Wimmer.** 1989. Proteolytic processing of polyproteins in the replication of RNA viruses. Biochemistry **28**:9881–9890.
10. **Hogle, J. M., M. Chow, and D. J. Filman.** 1985. Three-dimensional structure of poliovirus at 2.9 Å resolution. Science **229**:1358–1365.
11. **Jones, T. A.** 1985. Diffraction methods for biological macromolecules. Interactive computer graphics: FRODO. Methods Enzymol. **115**:157–171.
12. **Kirkegaard, K.** 1990. Mutations in VP1 of poliovirus specifically affect both encapsidation and release of viral RNA. J. Virol. **64**:195–206.
13. **Kitamura, N., B. L. Semler, P. G. Rothberg, G. R. Larsen, C. J. Adler, A. J. Dorner, E. A. Emini, R. Hanecak, J. J. Lee, S. van der Werf, C. W. Anderson, and E. Wimmer.** 1981. Primary structure, gene organization and polypeptide expression of poliovirus RNA. Nature (London) **291**:547–553.
14. **Kräusslich, H. G., C. Hölscher, Q. Reuer, J. Harber, and E. Wimmer.** 1990. Myristoylation of the poliovirus polyprotein is required for proteolytic processing of the capsid and for viral infectivity. J. Virol. **64**:2433–2436.
15. **Krishnaswamy, S., and M. G. Rossmann.** 1990. Structural refinement and analysis of mengo virus. J. Mol. Biol. **211**:803–844.
16. **Kunkel, T. A., R. M. Schaaper, E. James, and L. A. Loeb.** 1983. Infidelity of DNA replication as a basis of mutagenesis. Basic Life Sci. **23**:63–82.
17. **Larson, G. R., C. W. Anderson, A. J. Dorner, B. L. Semler, and E. Wimmer.** 1982. Cleavage sites within the poliovirus capsid protein precursors. J. Virol. **41**:340–344.
18. **Laemmli, U. K.** 1970. Cleavage of structural proteins during the assembly of the head of bacteriophage T4. Nature (London) **227**:680–685.
19. **Lee, C. K., and E. Wimmer.** 1988. Proteolytic processing of poliovirus polyprotein: elimination of 2A pro-mediated, alternative cleavage of polypeptide 3CD by in vitro mutagenesis. Virology **166**:405–414.
20. **Luo, M., G. Vriend, G. Kamer, I. Minor, E. Arnold, M. G. Rossmann, U. Boege, D. G. Scraba, G. M. Duke, and A. C. Palmenberg.** 1987. The atomic structure of mengo virus at 3.0 Å resolution. Science **235**:182–191.
21. **Murray, M. G., R. J. Kuhn, M. Arita, N. Kawamura, A. Nomoto, and E. Wimmer.** 1988. Poliovirus type 1/type 3 antigenic hybrid virus constructed in vitro elicits type 1 and type 3

neutralizing antibodies in rabbits and monkeys. Proc. Natl. Acad. Sci USA **85**:3203–3207.

22. **Rossmann, M. G., E. Arnold, J. W. Erikson, E. A. Frankenberger, J. P. Griffith, H.-J. Hecht, J. E. Johnson, G. Kamer, M. Luo, A. Mosser, R. Rueckert, B. Sherry, and G. Vriend.** 1985. Structure of a human common cold virus and functional relationship to other picornaviruses. Nature (London) **317**:145–153.
23. **Rossmann, M. G., and J. E. Johnson.** 1989. Icosahedral RNA virus structure. Annu. Rev. Biochem. **58**:533–573.
24. **Rueckert, R. R.** 1990. Picornaviridae and their replication, p. 507–547. *In* B. N. Fields (ed.), Virology. Raven Press, Ltd., New York.
25. **Sambrook, J., E. F. Fritsch, and T. Maniatis.** 1989. Molecular cloning: a laboratory manual, 2nd ed, p. 15.3–15.8. Cold Spring Harbor Laboratory Press, Cold Spring Harbor, N.Y.
26. **Semler, B. L., C. W. Anderson, N. Kitamura, P. G. Rothberg, W. L. Wishart, and E. Wimmer.** 1981. Poliovirus replication proteins: RNA sequence encoding P3-1b and the sites of proteolytic processing. Proc. Natl. Acad. Sci USA **78**:3464–3468.
27. **Semler, B. L., R. J. Kuhn, and E. Wimmer.** 1988. Replication of the poliovirus genome, p. 23–48. *In* E. Domingo, J. J. Holland, and P. Ahlquist (ed.), RNA genetics. CRC, Boca Raton, Fla.
28. **van der Werf, S., J. Bradley, E. Wimmer, F. W. Studier, and J. J. Dunn.** 1986. Synthesis of infectious poliovirus RNA by purified T7 RNA polymerase. Proc. Natl. Acad. Sci USA **83**:2330–2334.
29. **Zoller, M. J., and M. Smith.** 1984. Oligonucleotide-directed mutagenesis: a simple method using two oligonucleotide primers and a single-stranded DNA template. DNA **3**:479–488.